










Development of machine learning models for fractional flow reserve prediction in angiographically intermediate coronary lesions

Marco Lombardi MD¹  | Rocco Vergallo MD, PhD^{2,3} | Andrea Costantino MD⁴ |
Francesco Burzotta MD, PhD¹  | Tsunekazu Kakuta MD, PhD⁵  |
Tomasz Pawlowski MD, PhD⁶  | Antonio M. Leone MD, PhD¹  |
Gennaro Sardella MD, PhD⁷ | Pierfrancesco Agostoni MD, PhD⁸  |
Jonathan M. Hill MD⁹ | Giovanni L. De Maria MD, PhD¹⁰  |
Adrian P. Banning MD¹⁰ | Tomasz Roleder MD, PhD¹¹  |
Anouar Belkacemi MD, PhD¹² | Carlo Trani MD¹  | Francesco Burzotta MD, PhD¹

¹Department of Cardiovascular Sciences, Fondazione Policlinico Universitario A. Gemelli IRCCS, Università Cattolica Sacro Cuore, Rome, Italy

²Department of Internal Medicine and Medical Specialties (DIMI), Università di Genova, Genova, Italy

³Interventional Cardiology Unit, Cardiothoracic and Vascular Department (DICATOV), IRCCS Ospedale Policlinico San Martino, Genova, Italy

⁴Department of Biomedical Sciences, Humanitas University, Milan, Italy

⁵Department of Cardiovascular Medicine, Tsuchiura Kyodo General Hospital, Tsuchiura, Japan

⁶Department of Cardiology, Central Hospital of Internal Affairs and Administration Ministry, Postgraduate Medical Education Centre, Warsaw, Poland

⁷Department of Cardiovascular Sciences, Policlinico Umberto I, Sapienza University of Rome, Rome, Italy

⁸HartCentrum, Ziekenhuis Netwerk Antwerpen (ZNA) Middelheim, Antwerp, Belgium

⁹Royal Brompton Hospital, London, UK

¹⁰Oxford Heart Centre, John Radcliffe Hospital, Oxford University Hospitals, NHS Foundation Trust, Oxford, UK

¹¹Department of Cardiology, Hospital Wroclaw, Wroclaw, Poland

¹²Department of Cardiology, AZ West Hospital, Veurne, Belgium

Correspondence

Francesco Burzotta, MD, PhD, Department of Cardiovascular Sciences, Fondazione Policlinico Universitario A. Gemelli IRCCS, Università Cattolica del Sacro Cuore, Largo A. Gemelli, 8-00168 Rome, Italy.
Email: francesco.burzotta@unicatt.it

Abstract

Background: Fractional flow reserve (FFR) represents the gold standard in guiding the decision to proceed or not with coronary revascularization of angiographically intermediate coronary lesion (AICL). Optical coherence

Abbreviations: %AS, area stenosis; ACS, acute coronary syndrome; AICL, angiographically intermediate coronary lesions; AUC, area under the curve; CABG, coronary artery by-pass graft; CART, classification and regression tree; DS, diameter stenosis; FFR, fractional flow reserve; IVUS, intravascular ultrasound; kNN, k-nearest neighbor; LL, lesion length; MI, myocardial infarction; ML, machine learning; MLA, minimum lumen area; MLD, minimum lumen diameter; NPV, negative predictive value; OCT, optical coherence tomography; PCI, percutaneous coronary intervention; PDA, penalized discriminant analysis; PPV, positive predictive value; QCA, quantitative coronary angiography; RD, reference diameter; RF, random forest; SVM, support vector machines; XGB, extreme gradient boosting.

Registration: URL: <https://www.clinicaltrials.gov>; Unique identifier: NCT03573388.

Marco Lombardi and Rocco Vergallo contributed equally to this work.

This is an open access article under the terms of the [Creative Commons Attribution-NonCommercial-NoDerivs](https://creativecommons.org/licenses/by-nc-nd/4.0/) License, which permits use and distribution in any medium, provided the original work is properly cited, the use is non-commercial and no modifications or adaptations are made.

© 2024 The Author(s). *Catheterization and Cardiovascular Interventions* published by Wiley Periodicals LLC.

tomography (OCT) allows to carefully characterize coronary plaque morphology and lumen dimensions.

Objectives: We sought to develop machine learning (ML) models based on clinical, angiographic and OCT variables for predicting FFR.

Methods: Data from a multicenter, international, pooled analysis of individual patient's level data from published studies assessing FFR and OCT on the same target AICL were collected through a dedicated database to train ($n = 351$) and validate ($n = 151$) six two-class supervised ML models employing 25 clinical, angiographic and OCT variables.

Results: A total of 502 coronary lesions in 489 patients were included. The AUC of the six ML models ranged from 0.71 to 0.78, whereas the measured F1 score was from 0.70 to 0.75. The ML algorithms showed moderate sensitivity (range: 0.68–0.77) and specificity (range: 0.59–0.69) in detecting patients with a positive or negative FFR. In the sensitivity analysis, using 0.75 as FFR cut-off, we found a higher AUC (0.78–0.86) and a similar F1 score (range: 0.63–0.76). Specifically, the six ML models showed a higher specificity (0.71–0.84), with a similar sensitivity (0.58–0.80) with respect to 0.80 cut-off.

Conclusions: ML algorithms derived from clinical, angiographic, and OCT parameters can identify patients with a positive or negative FFR.

KEYWORDS

artificial intelligence, fractional flow reserve, intermediate coronary lesions, machine learning, optical coherence tomography

1 | INTRODUCTION

According to current international guidelines, fractional flow reserve (FFR) is the gold standard in deciding whether to perform coronary revascularization in patients with angiographically intermediate coronary lesions (AICL).^{1,2} Intravascular imaging with optical coherence tomography (OCT) is commonly performed to characterize coronary plaque morphology (especially the presence of signs of vulnerability) and to guide the optimization of percutaneous coronary intervention (PCI) results,^{3–7} especially when facing complex lesions, such as bifurcations.⁸ Recently, a randomized clinical trial⁹ demonstrated that OCT is a valuable option over FFR in the management of AICL. The association between FFR for functional assessment and OCT for optimization of PCI could be a perfect combination. However, in the “real world,” the use of both techniques during a single procedure would collide with an increase in procedural costs and time. Machine learning (ML) algorithms allow computers to learn from data and experience, and to make predictions about previously unanalyzed variables.^{10–13} ML models have recently demonstrated excellent performance in the analysis of cardiovascular multislice computed-tomography (MSCT), with the goal of improving outcomes prediction.¹⁴ This is due to their ability to select and weigh individual imaging features and to identify multidimensional relationship between them. Classical limitations of building predictive models from traditional statistical methods are represented by the presence of too many

predictors, nonlinear associations between factors and outcomes, and multiple interactions between variables. ML could be used to improve current modeling by making a more accurate and precise predictions for the outcomes of interest. The aim of the present study was to develop, on the basis of clinical, angiographic, and OCT parameters, different ML models capable of classifying AICL into those with a positive FFR (≤ 0.80) and those with a negative FFR (> 0.80).

2 | METHODS

This study complies with the guidelines for Transparent Reporting of a Multivariable Prediction Model for Individual Prognosis or Diagnosis (TRIPOD)¹⁵ (Supporting Information S1: Table 2).

2.1 | Study population

This was a post-hoc analysis of the multicentric OMEF study (NCT03573388). Patient data were pooled from studies conducted at eight centers across Europe (Italy, United Kingdom, Poland, Netherlands) and Japan, that agreed to data sharing.^{16–23} Patients with acute or chronic coronary syndrome and angiographic evidence of at least one AICL (defined as visual diameter stenosis between

30% and 80%) in whom both FFR and OCT had been performed were included. Principal investigators were asked to complete a structured database by providing a series of anonymized clinical, angiographic, OCT, and FFR data. Individual study protocols and ethical aspects have been reported in each study.¹⁶⁻²³

2.2 | Quantitative coronary angiography for coronary lesion assessment

Quantitative coronary angiography (QCA) analyses were performed offline with validated software on a single, selected 2D end-diastolic image frame. Reference vessel diameters were based on the computer estimation of the original arterial dimensions at the stenosis site. The following angiographic parameters were calculated and expressed as absolute values (mm): minimal lumen diameter (MLD), proximal and distal reference diameter (RD) and lesion length (LL). Diameter stenosis (DS) was derived from the previously collected angiographic parameters and expressed as a percentage.

2.3 | Fractional flow reserve

Technical assessment of FFR was performed using different systems according to the operator's discretion and/or study protocol. After the placement of a guide catheter at the coronary ostium, a 0.014-inch pressure monitoring guidewire was advanced beyond the target AICL under fluoroscopic examination. Then, FFR was defined as the lowest ratio of distal coronary pressure divided by aortic pressure after achievement of hyperemia using intracoronary or endovenous adenosine according to local practice at each center.²⁴ FFR > 0.80 was defined as "negative," and in these cases, according to guidelines, myocardial revascularization was deferred.

2.4 | Optical coherence tomography

Target AICLs where FFR was performed underwent OCT evaluation (after intracoronary administration of nitroglycerin). The OCT catheter was advanced to the distal end of the target AICL and the entire length of the region of interest was scanned. Commercially available software were used for analyses as reported in the original studies, and the following parameters were collected: minimum lumen area (MLA, defined as cross-sectional area at the smallest luminal area level), proximal reference lumen area (RLA, defined as the cross-section at the frame with largest lumen within 10 mm proximal to MLA and before any major side branch), distal RLA (defined as the cross-section at the frame with largest lumen within 10 mm distal to MLA and before any major side branch), and mean RLA (defined as [proximal RLA + distal RLA]/2). Based on these parameters, percentage of area stenosis (%AS) was calculated using the following formula: [(mean RLA-MLA)/mean RLA] x 100. Plaque rupture (i.e., ulceration) was defined as a recess in the plaque

beginning at the luminal-intimal border. Plaque thrombus included both red thrombus (intraluminal mass with high backscatter and high attenuation) and white thrombus (intraluminal mass with high backscatter and low attenuation). Quantitative and qualitative parameters were in accordance with the consensus document from the International Working Group for intravascular OCT (IWG-IVOCT) standardization and validation.²⁵

2.5 | Data collection and preprocessing

The variables included in the analysis were: age, gender, smoking, hypertension, diabetes mellitus, dyslipidemia, previous (>1 month) or recent (within 1 month) acute coronary syndrome (ACS), previous PCI and coronary artery bypass grafting (CABG), coronary vessel evaluated, QCA parameters (proximal and mean RD, LL, MLD, %DS), and OCT parameters (proximal and distal RLA, LL, MLA, %AS, thrombus, ulceration, MLA < 2.0 mm², %AS > 73%). In addition to the continuous variables, the prespecified cut-off values adopted for MLA and %AS were derived from the main analysis of the OMEF study.²⁶ Missing data for variables of interest were analyzed and categorized as "missing completely at random," "missing at random," and "not missing at random." Overall, missing values accounted for 2.9% of all datasets. Variables found to be missing at random were imputed using a linear or a logistic regression method for continuous and categorical variables, respectively.^{27,28} The data set was randomly split using a 70:30 ratio, whereby the ML algorithm was trained on 70% of the available cases (training data set) and tested on the remaining 30% (testing data set). After the splitting process, the proportion of FFR positive and negative for the target AICLs was maintained.

2.6 | Model training and validation

Six 2-class supervised ML decision models, which were selected as the current and most common predictive model types in the literature, were used to predict the presence of positive FFR (FFR ≤ 0.80) or negative FFR (FFR > 0.80) for the target AICLs. In particular, the training data set was used to train the following six ML-based models: classification and regression tree (CART),²⁹ k-nearest neighbor (kNN),³⁰ penalized discriminant analysis (PDA),³¹ random forest (RF),³² support vector machines (SVM),³³ and extreme gradient boosting (XGB).³⁴ To ensure model stability and reduce bias, a repeated 10-fold cross-validation was performed during the training of all ML algorithms. A data set augmentation technique (Synthetic Minority Oversampling Technique or SMOTE) was adopted during the training process to generate more samples for the minority class to correct for class imbalance.³⁵ Random hyperparameter tuning was performed to maximize the area under the receiver operating characteristic (ROC) curve.³⁶ The classification performance of the ML algorithms was measured on the testing data by comparing accuracy, area under the curve (AUC), sensitivity, specificity, positive predictive value (PPV), negative predictive value (NPV), and F1

score (a standard metric for ML classifiers combining precision and recall). A positive FFR (≤ 0.80) was labeled as "positive" class for the classification algorithms. Next, the results were plotted using ROC curves. As per sensitivity purpose, we also repeated the same analysis labeling $\text{FFR} \leq 0.75$ as positive and $\text{FFR} > 0.75$ as negative, and excluding patients with ACS. The testing data set was used to calculate a permutation feature importance (PFI) score (a measure of the reduction in model performance when the value of a single feature is randomly shuffled) that was used to identify the variables with the greatest impact on model prediction.³⁷ Specifically, PFI scores were calculated as the difference in AUC model performance before and after altering a particular independent variable.

2.7 | Statistical analysis

Categorical variables were expressed as counts (percentages) and compared using the χ^2 or Fisher's exact test. After assessing data distribution using the Kolmogorov–Smirnov test, continuous variables were expressed as mean \pm standard deviation or median (interquartile range) and compared using the independent samples Student's *t*-test or the Mann–Whitney U test, according to the distribution. The accuracy, AUC, sensitivity, specificity, PPV, NPV, and F1 scores of the six ML models were measured. Statistical analyses were performed using the R software for statistical computing (R version 4.0.1, Foundation for Statistical Computing) and SPSS v.28.0 (IBM Corp). A value of $p < 0.05$ was considered to indicate statistical significance.

3 | RESULTS

3.1 | Baseline characteristics

The final study population comprised a total of 502 AICLs in 489 patients. Baseline patients' characteristics are summarized in Table 1. The mean age was 65 years, and the clinical presentation was chronic coronary syndrome in the vast majority of the patients (about 90%). The target vessel location was left anterior descending artery (LAD) in 311 lesions (62%), left circumflex artery (LCx) in 72 lesions (14%), and right coronary artery (RCA) in 119 lesions (24%).

3.2 | QCA and OCT parameters

QCA and OCT parameters of AICL stratified according to the FFR values (≤ 0.80 or > 0.80) are reported in Table 2. At QCA, with respect to those with negative FFR, target AICLs lesion with $\text{FFR} \leq 0.80$ were found to have a significantly greater lesion length (15.2 ± 8.8 vs. 12.5 ± 6.0 mm; $p < 0.001$) and %DS (58.7 ± 12.4 vs. 51.0 ± 12.5 ; $p < 0.001$), whereas minimum lumen diameter (1.08 ± 0.37 vs. 1.47 ± 0.46 mm; $p < 0.001$) and mean reference diameter (2.65 ± 0.62 vs. 3.05 ± 0.73 mm; $p < 0.001$) were significantly smaller. At OCT similar data were observed in the

TABLE 1 Baseline clinical characteristics.

	Overall population (489 patients)
Age, years	65.2 \pm 10.4
Male sex	368 (75.3)
Hypertension	322 (65.8)
Dyslipidemia	279 (57.1)
Diabetes mellitus	150 (30.7)
Current smoking	121 (24.7)
Family history	40 (8.2)
Clinical presentation	
Acute coronary syndrome	55 (11.2)
Chronic coronary syndrome	434 (88.8)
Previous myocardial infarction	132 (27.0)
Previous percutaneous coronary interventions	234 (47.9)
Previous coronary artery by-pass surgery	8 (1.6)

Note: Data are expressed as counts (percentages) or mean \pm standard deviation.

positive FFR group, with a significantly smaller MLA (1.55 ± 0.85 vs. 2.91 ± 1.64 mm; $p < 0.001$), while lesion length (15.0 ± 6.6 vs. 12.7 ± 6.2 mm; $p < 0.001$), and % AS (75.5 ± 11.7 vs. 60.8 ± 20.4 , $p < 0.001$) were significantly greater respect to AICLs with negative FFR. No statistically significant differences were observed in the prevalence of OCT-detected ulceration and thrombus between the two groups.

3.3 | Performance of ML models

The data set was randomly divided into a training data set and a testing data set consisting of 351 (70%) and 151 (30%) patients, respectively (Central Illustration– Figure 1). The development of ML models was performed on the training data set using the 25 available variables abovementioned. Then, each trained model was applied to the testing data set to predict the presence of a positive or negative FFR. Table 3 shows the confusion matrix containing the information of correct and incorrect predictions of each model compared to the actual class. Table 4 summarizes the classification performance of each prediction algorithm. Overall, the AUC of the six ML models ranged from 0.71 to 0.78, whereas the F1 score was between 0.70 and 0.75. The accuracy was moderate and varied between 0.66 and 0.70, in fact ML algorithms showed a mild higher sensitivity (range: 0.68–0.77) rather than specificity (range: 0.59–0.69) in detecting patients with positive or negative FFR. Accordingly, PPV measured was higher (range: 0.71–0.75) than NPV (range: 0.59–0.66). The ROC curves and the PFI scores of the six ML-developed models are shown

TABLE 2 QCA and OCT findings in AICL with positive or negative FFR.

	FFR ≤ 0.80 (289 lesions)	FFR > 0.80 (213 lesions)	p- value
Lesion location			
LAD	199 (68.9)	112 (52.6)	
LCx	32 (11.1)	40 (18.8)	0.001
RCA	58 (20.1)	61 (28.6)	
QCA parameters			
Lesion length, mm	15.2 ± 8.8	12.5 ± 6.0	<0.001
MLD, mm	1.08 ± 0.37	1.47 ± 0.46	<0.001
Mean RD, mm	2.65 ± 0.62	3.05 ± 0.73	<0.001
%DS	58.7 ± 12.4	51.0 ± 12.5	<0.001
OCT parameters			
Lesion length, mm	15.0 ± 6.6	12.7 ± 6.2	<0.001
MLA, mm ²	1.55 ± 0.85	2.91 ± 1.64	<0.001
%AS, %	75.5 ± 11.7	60.8 ± 20.4	<0.001
Ulceration	31 (11.6)	23 (10.8)	0.805
Thrombus	13 (4.5)	10 (4.7)	0.917

Note: Data are expressed as counts (percentages) or mean ± standard deviation.

Abbreviations: AICL, angiographically-intermediate coronary lesions; DS, diameter stenosis; FFR, fractional flow reserve; LAD, left anterior descending; LCx, left circumflex; MLA, minimum lumen area; MLD, minimum lumen diameter; OCT, optical coherence tomography; QCA, quantitative coronary angiography; RCA, right coronary artery; RD, reference diameter; %AS, percentage area stenosis.

respectively in Figures 2 and 3. Variables contributing to the model are displayed in descending order according to their corresponding importance scores. The absolute magnitude of a PFI score reflects the impact of a single variable on the overall performance. In the sensitivity analysis, using 0.75 as FFR cut-off, we found higher AUC (0.78–0.86). Specifically, the models showed higher accuracy (0.72–0.81) and specificity (0.71–0.84), but with a similar sensitivity (0.58–0.80) respect to 0.80 cut-off (Table 5; and Supporting Information S1: Table 3).

Additionally, in the sensitivity analysis excluding patients with ACS we found an AUC ranging from 0.73 to 0.82 with an accuracy between 0.64 and 0.76 (Supporting Information S1: Tables 4–5).

4 | DISCUSSION

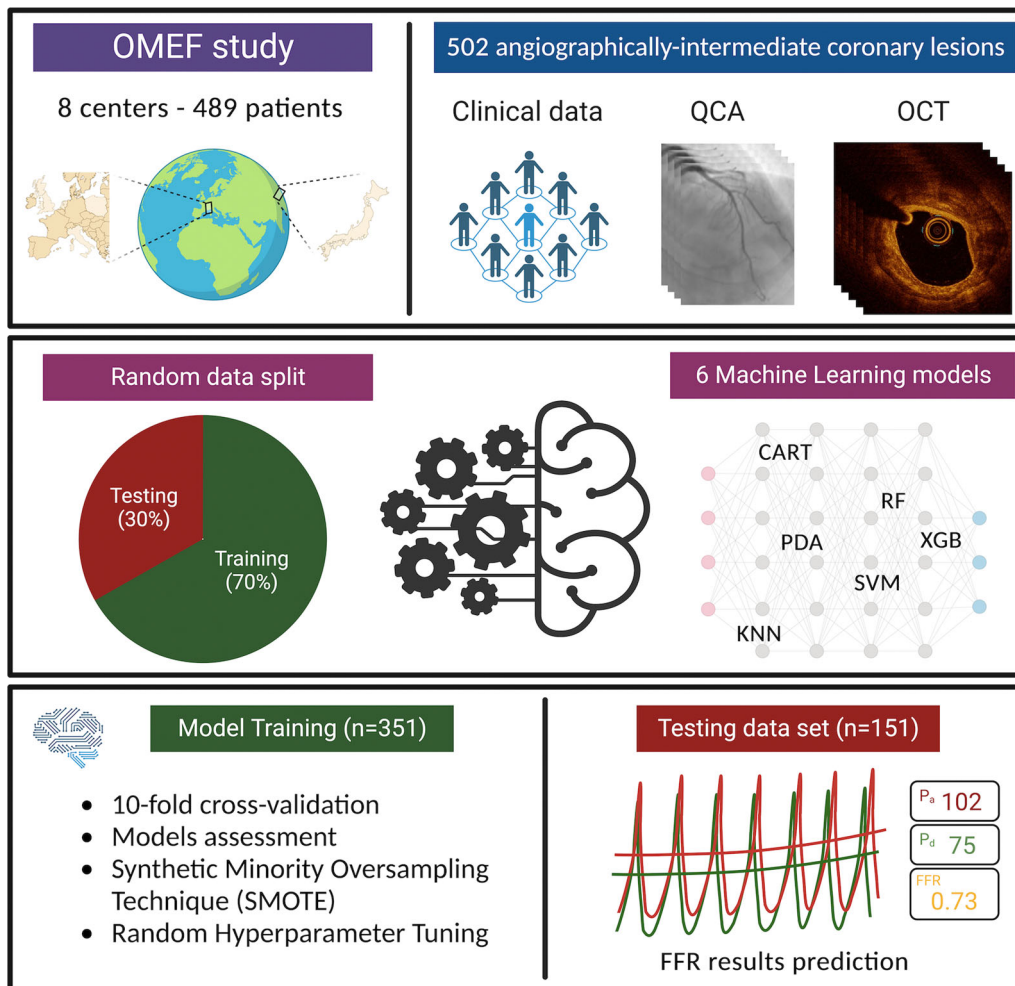
The assessment of the functional significance of AICLs is recommended by international guidelines when dealing with the decision to perform coronary revascularization.^{1,38} On the other hand, OCT is usually used to characterize coronary morphology by providing

invaluable information about plaque composition and vulnerability. In recent years, several attempts have been made to implement image-based mathematical models to predict the presence of myocardial ischemia, such as quantitative flow ratio (QFR) derived from 3D-QCA computational fluid dynamics models³⁹ or an OCT-based FFR (OFR) computational approach.⁴⁰ Hence, we assumed that OCT may therefore provide additional insights about the functional significance of AICL in addition to clinical and angiographic findings. To the best of our knowledge, this is the first international multicenter study focused on the development of ML algorithms that integrate clinical, QCA and OCT data for the prediction of FFR results. In the present post-hoc analysis of the OMEF study,²⁶ which includes OCT and FFR data obtained in the same target AICLs, six ML algorithms were trained and tested in a multi-center cohort of 489 patients (502 coronary lesions). The main findings of this study were:

- the feasibility of the application of ML models to identify patients with a positive or negative FFR, as their classification performance showed an AUC between 0.71 and 0.78 which increased when considering 0.75 as cut-off (AUC range: 0.78–0.86);
- overall, the ML models demonstrated moderate sensitivity (range: 0.68–0.77) and specificity (range: 0.59–0.69) for 0.80 cut-off and a good sensitivity (range: 0.58–0.80) and specificity (range: 0.71–0.84) for 0.75 cut-off.

The classification performance of the ML algorithms should be analyzed according to the specific clinical context. Models with either high sensitivity or high specificity should be preferred depending on the specific clinical setting. A higher sensitivity of ML models may allow the identification of patients with a high probability of hemodynamically significant AICL. In this way, the ML models may be a supportive tool for physicians to identify patients requiring revascularization of an AICL, at the expense of possible misclassifications of patients with functional significant AICLs despite a negative FFR invasive assessment. Although our model achieved an AUC of 0.71–0.78, indicating moderate to high classification accuracy, there is potential for further enhancement. Future studies should focus on refining the developed models to improve their accuracy and further evaluate their clinical applicability in the decision-making process.

A PFI score was also calculated using the testing data set to identify the key variables used in the different ML models.³⁷ Overall, MLA was confirmed to be the most important predictor of a positive FFR. In addition, other variables influenced the classification performance, such as age, dyslipidemia, coronary vessel evaluated, previous MI, MLA < 2.0 mm², MLD, proximal RLA and RD, %AS, or % DS, although heterogeneous results were found between the developed ML models. Of note, PFI score is calculated to describe the algorithm used by each ML model. However, the overall interpretability of the analysis remains uncertain because the meaning of the score is still unclear, and the only reliable information about each input variable is its ranking. These signals suggest that a comprehensive assessment of vessel geometry might generate an accurate prediction of FFR.



CENTRAL ILLUSTRATION. FIGURE 1 Flow chart of the machine learning (ML) methodology. Illustration created with BioRender. com. [Color figure can be viewed at wileyonlinelibrary.com]

The present study utilizes data from the multicenter OMEF study, encompassing patients from five countries across Europe and Asia. This diverse data set allows for consideration of different clinical settings and potential racial influences, providing a more comprehensive evaluation of the model's performance. Nonetheless, external validation in additional populations is crucial to confirm the generalizability and robustness of these models.

The ischemic threshold for FFR that defines significant ischemia prompting the decision toward coronary revascularization is still today matter of debate; hence some have defined the range 0.75–0.80 as a “gray zone.”⁴¹ In a large meta-analysis revascularization of coronary stenoses with gray zone FFR showed no advantage over a deferral strategy in terms of MACE.⁴² Indeed, in a previous IVUS study authors developed six ML models for FFR prediction (accuracy ranging from 0.80 to 0.83), which enhanced predictive power after the exclusions of lesions with a borderline FFR (0.75–0.80).⁴³ In this fashion, we performed a sensitivity analysis using a different FFR cut-off (≤ 0.75), which reported a higher accuracy and specificity, but with a quite similar sensitivity. In addition, we retained lesions from the gray zone because our main aim was to

evaluate the feasibility of using ML models to predict positive or negative FFR in clinical practice for all patients tackled with AICL. Although the results obtained with 0.75 as ischemic cut-off are encouraging, we preferred to report them only as additional analyses because the current cut-off derived from FAME 2 trial⁴⁴ used in clinical practice is 0.80 and the present post-hoc analysis was not designed to propose the application of a different cut-off. An ongoing large, multicentric international intravascular imaging and pressure wire trial (COMBINE-INTERVENE trial) will provide definitive insights into this issue combining a lower ischemic cut-off threshold (0.75) with OCT characteristics of plaque vulnerability for coronary revascularization.

In the sensitivity analysis excluding patients with ACS we found an AUC ranging from 0.73 to 0.82 with an accuracy between 0.64 and 0.76. Whether these improved results are due to better classification of the model outside the context of ACS or to overfitting related to the reduced number of patients included^{45,46} is unknown, especially since the main analysis acknowledges the presence of ACS among the 25 variables. Further studies are needed to answer this specific question.

Recently, computational methods have emerged for deriving FFR values from OCT, showcasing a good correlation with invasive FFR.^{40,47,48} Conversely, ML models developed in this post-hoc analysis of the OMEF study exhibit the ability to seamlessly integrate data from various sources, such as intracoronary imaging, coronary angiography, and patient clinical characteristics. The clinical application of ML models presents a more user-friendly interface for interventional cardiologists, also circumventing additional computational time as it only requires the inference time of the included variables. Despite the study's limitation of lacking qualitative data from OCT, this can also be viewed as a strength. The majority of OCT features utilized in developing the six ML algorithms are effortlessly and swiftly generated, and many are already assessed by operators,

with new-generation intracoronary tools automating the generation of crucial information such as MLA and %AS. In a new era of personalized medicine, there is a growing demand for more accurate risk prediction tailored to the patient. The use of ML models may allow interventional cardiologists to interact with inputs for individualized prediction, and to explore the impact of specific features available from angiography in combination with OCT on ischemia risk.

4.1 | Limitations

Our study has several limitations. First, it was a retrospective study and therefore subject to potential selection bias. Second, although qualitative analysis of coronary lesions provides important information related to clinical outcomes (e.g., thin-cap fibroatheroma and/or

TABLE 3 Confusion matrices of the ML models (FFR cut-off 0.80).

Model	Predicted class	Actual class (n = 151)	
		FFR > 0.80 (n = 64)	FFR ≤ 0.80n (n = 87)
CART	FFR > 0.80	39	20
	FFR ≤ 0.80	25	67
KNN	FFR > 0.80	38	22
	FFR ≤ 0.80	26	65
PDA	FFR > 0.80	44	28
	FFR ≤ 0.80	20	59
RF	FFR > 0.80	41	22
	FFR ≤ 0.80	23	65
SVM	FFR > 0.80	38	22
	FFR ≤ 0.80	26	65
XGB	FFR > 0.80	41	28
	FFR ≤ 0.80	23	59

Abbreviations: CART, classification and regression tree; FFR, fractional flow reserve; kNN, k- nearest neighbor; ML, machine learning; PDA, penalized discriminant analysis; RF, random forest; SVM, support vector machine; XGB, extreme gradient boosting.

TABLE 4 Classification performance of the ML models (FFR cut-off 0.80).

Model	AUC	F1 score	Accuracy	Sensitivity	Specificity	PPV	NPV
CART	0.71	0.75	0.70	0.77	0.61	0.73	0.66
KNN	0.73	0.73	0.68	0.75	0.60	0.71	0.63
PDA	0.75	0.71	0.68	0.68	0.69	0.75	0.61
RF	0.78	0.74	0.70	0.75	0.64	0.74	0.65
SVM	0.74	0.73	0.68	0.75	0.59	0.71	0.63
XGB	0.75	0.70	0.66	0.68	0.64	0.72	0.59

Abbreviations: AUC, area under the curve; CART, classification and regression tree; kNN, k- nearest neighbor; NPV, negative predictive value; PDA, penalized discriminant analysis; PPV, positive predictive value; RF, random forest; SVM, support vector machine; XGB, extreme gradient boosting.

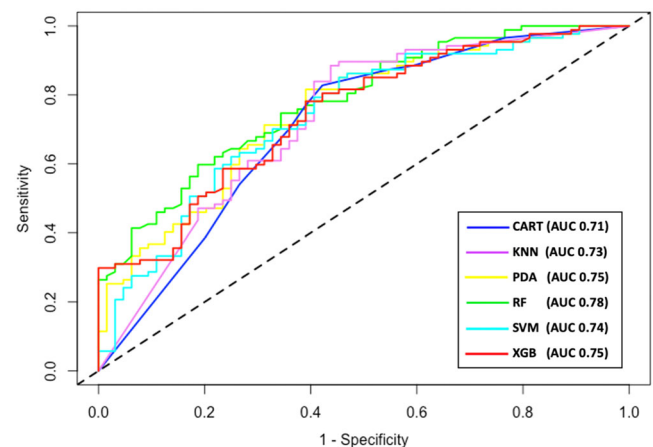


FIGURE 2 ROC curves showing the accuracy in the prediction of a positive or negative FFR. The diagonal line (black) represents the identity line (no discrimination line). CART, classification and regression tree; kNN, k- nearest neighbor; PDA, penalized discriminant analysis; RF, random forest; SVM, support vector machine; XGB, extreme gradient boosting. [Color figure can be viewed at wileyonlinelibrary.com]

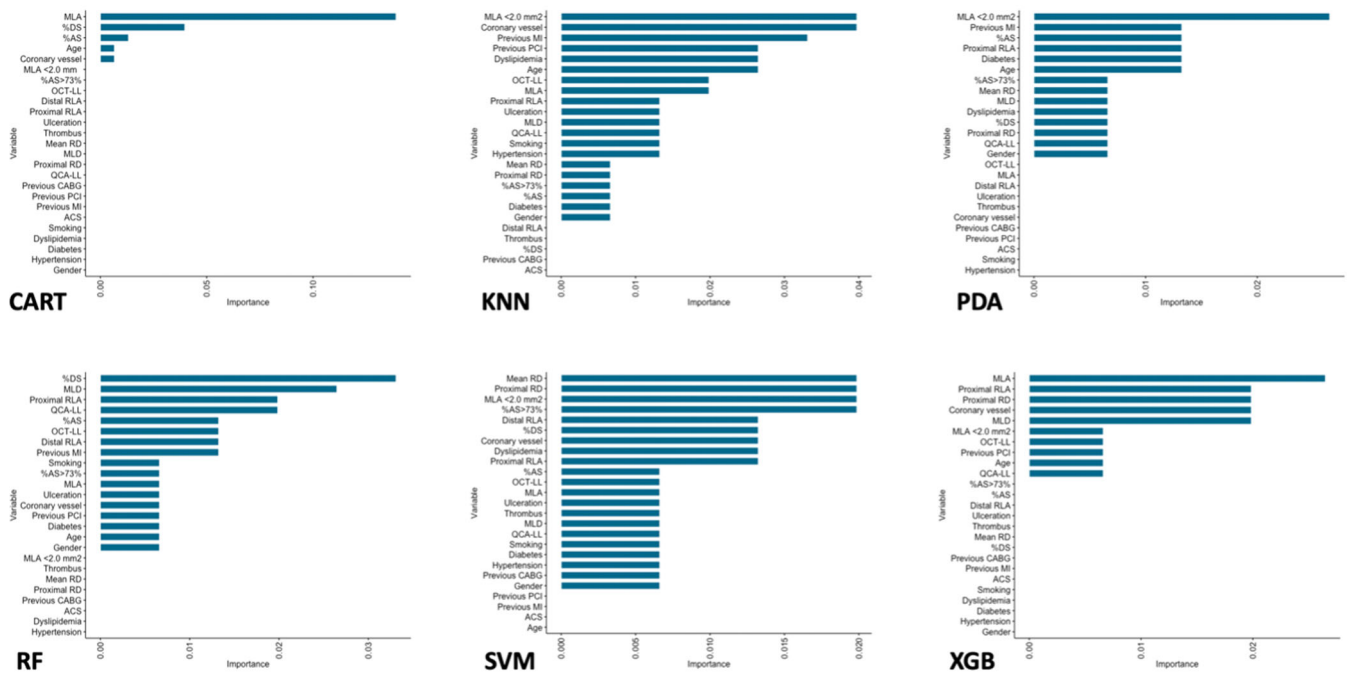


FIGURE 3 Permutation feature importance scores of the six ML models. Variables are displayed in descending order according to their corresponding importance score. ACS, acute coronary syndrome; CABG, coronary artery by-pass grafting; CART, classification and regression tree; kNN, k-nearest neighbor; MI, myocardial infarction; MLA, minimum lumen area; MLD, minimum lumen diameter; OCT-LL; optical coherence tomography lesion length; PCI, percutaneous coronary intervention; PDA, penalized discriminant analysis; QCA-LL, quantitative coronary angiography lesion length; RD, reference diameter; RF, random forest; SVM, support vector machine; XGB, extreme gradient boosting; %AS, percentage area stenosis; %DS, percentage diameter stenosis. [Color figure can be viewed at wileyonlinelibrary.com]

TABLE 5 Classification performance of the ML models (FFR cut-off 0.75).

Model	AUC	F1 score	Accuracy	Sensitivity	Specificity	PPV	NPV
CART	0.78	0.66	0.72	0.74	0.71	0.59	0.83
KNN	0.84	0.63	0.75	0.58	0.84	0.68	0.78
PDA	0.85	0.74	0.79	0.84	0.76	0.67	0.89
RF	0.86	0.76	0.81	0.80	0.82	0.72	0.88
SVM	0.81	0.65	0.75	0.64	0.82	0.67	0.80
XGB	0.85	0.71	0.78	0.74	0.80	0.68	0.85

Abbreviations: AUC, area under the curve; CART, classification and regression tree; kNN, k-nearest neighbor; NPV, negative predictive value; PDA, penalized discriminant analysis; PPV, positive predictive value; RF, random forest; SVM, support vector machine; XGB, extreme gradient boosting.

macrophage infiltration), we did not include these parameters in the analysis because of a lack of data from the original database. Further studies will be needed to address these important features. Third, the lack of transparency in the analysis could be associated with a difficult interpretation of the process, as previously described.⁴⁹ Predictions models generated by the ML algorithm are based on multiple layers of analysis, but the specific process is not directly accessible and the effects of each variable and the relationship between them cannot be presented in a clear format. In particular, ML does not generate measures of the effect size of individual variables, as instead defined by the odds ratio of a multivariable logistic regression model. Notably, the absolute value of the PFI score

does not give information regarding the real impact of the model prediction, but it can only be used to give a ranking between variables in terms of importance.^{37,50,51} Further research is needed to validate the clinical utility of these scores and to develop more interpretable models or supplementary tools to aid clinicians in utilizing ML insights effectively. ML algorithms can identify complex patterns of nonlinear combinations of the input variables to improve classification performance. However, future studies should also focus on a better categorization of the included variables to improve the interpretability of these algorithms. Fourth, another limitation of our study is the higher prevalence of LAD intermediate lesions, which may limit the generalizability of our results to lesions located in the RCA and LCx

arteries. Fifth, the lack of external validation is a limitation of the present analysis, and future studies should focus on validating these findings in diverse clinical environments to ensure their broad applicability and reliability in clinical practice.

A final important limitation of this post-hoc analysis of the OMEF study is that binary classifiers cannot be translated into continuous hemodynamic indexes, thereby reducing the information provided by these variables, and potentially underestimating the accuracy of the developed models.

5 | CONCLUSIONS

The observations collected in this post-hoc analysis of the OMEF collaborative study suggest that machine learning-derived algorithms based on clinical, angiographic, and OCT parameters can identify patients with a positive or negative FFR. These preliminary findings suggest that ML algorithms might allow the selection of patients with positive or negative FFR without the need for an invasive intracoronary functional assessment. Appropriately designed prospective studies with a larger sample size are warranted to further determine FFR prediction.

ACKNOWLEDGMENTS

BioRender platform and templates were used for creating the central illustration. The study has been partially supported by Abbott in the organization phase. The company has been not involved in the study conduction nor in results interpretation. Open access publishing facilitated by Universita Cattolica del Sacro Cuore, as part of the Wiley - CRUI-CARE agreement.

CONFLICT OF INTEREST STATEMENT

Marco Lombardi is supported by a grant from Fondazione Enrico ed Enrica Sovena (Rome, Italy). Rocco Vergallo received speaker fees from Abbott Vascular and Terumo. Francesco Bianchini receives a research grant from Abbott Vascular. Tomasz Pawlowski received a speaker fee from Abbott Vascular, Philips IGT. Antonio Maria Leone is an advisor for Abbott Vascular and Bracco Imaging and received speaking honoraria from Abbott Vascular, Medtronic and Abiomed in the past. Jonathan Hill received speaker fees, honoraria and consulting fees from Abbott Vascular, Abiomed, Boston Scientific, Shockwave, and Equity Shockwave. Giovanni Luigi De Maria received a speaker fee from Abbott Vascular, consultancy fees from Miracor Medical SA, and a research grant from Abbott Vascular, Philips, Medtronic, Terumo, Opsens and Miracor Medical SA. Carlo Trani and Francesco Burzotta received speakers' fees from Abbott Vascular, Abiomed, Medtronic and Terumo. The other authors have no conflict of interest to disclose in relation to the present manuscript.

DATA AVAILABILITY STATEMENT

The data that support the findings of this study are available on request from the corresponding author. The data are not publicly available due to privacy or ethical restrictions.

ORCID

Marco Lombardi  <http://orcid.org/0000-0002-4045-2859>
 Francesco Bianchini  <http://orcid.org/0000-0001-9043-6462>
 Tsunekazu Kakuta  <http://orcid.org/0000-0002-4004-5292>
 Tomasz Pawlowski  <http://orcid.org/0000-0002-0827-6373>
 Antonio M. Leone  <https://orcid.org/0000-0002-1276-9883>
 Pierfrancesco Agostoni  <http://orcid.org/0000-0002-1505-9369>
 Giovanni L. De Maria  <https://orcid.org/0000-0003-3572-1855>
 Tomasz Roleder  <http://orcid.org/0000-0002-1370-7369>
 Carlo Trani  <http://orcid.org/0000-0001-9777-013X>

REFERENCES

1. Writing Committee Members, Tamis-Holland JE, Lawton, JS, Bangalore S, et al. 2021 ACC/AHA/SCAI guideline for coronary artery revascularization. *J Am Coll Cardiol*. 2022;79(2):e21-e129. doi:10.1016/j.jacc.2021.09.006
2. Neumann FJ, Sousa-Uva M. Ten commandments for the 2018 ESC/EACTS guidelines on myocardial revascularization. *Eur Heart J*. 2019;40(2):79-80. doi:10.1093/eurheartj/ehy855
3. Wijns W, Shite J, Jones MR, et al. Optical coherence tomography imaging during percutaneous coronary intervention impacts physician decision-making: ILUMIEN I study. *Eur Heart J*. 2015;36(47):3346-3355. doi:10.1093/eurheartj/ehv367
4. Maehara A, Ben-Yehuda O, Ali Z, et al. Comparison of stent expansion guided by optical coherence tomography versus intravascular ultrasound: the ILUMIEN II study (Observational Study of Optical Coherence Tomography [OCT] in Patients Undergoing Fractional Flow Reserve [FFR] and Percutaneous Coronary Intervention). *JACC: Cardiovasc Interv*. 2015;8(13):1704-1714. doi:10.1016/j.jcin.2015.07.024
5. Ali ZA, Maehara A, G en ereux P, et al. Optical coherence tomography compared with intravascular ultrasound and with angiography to guide coronary stent implantation (ILUMIEN III: OPTIMIZE PCI): a randomised controlled trial. *The Lancet*. 2016;388(10060):2618-2628. doi:10.1016/S0140-6736(16)31922-5
6. Jones DA, Rathod KS, Koganti S, et al. Angiography alone versus Angiography Plus optical Coherence Tomography to guide Percutaneous Coronary Intervention. *JACC: Cardiovasc Interv*. 2018;11(14):1313-1321. doi:10.1016/j.jcin.2018.01.274
7. Burzotta F, Trani C. Intracoronary imaging. *Circ Cardiovasc Interv*. 2018;11(11):e007461. doi:10.1161/CIRCINTERVENTIONS.118.007461
8. Holm NR, Andreasen LN, Neghabat O, et al. OCT or angiography guidance for PCI in complex bifurcation lesions. *N Engl J Med*. 2023;389(16):1477-1487. doi:10.1056/NEJMoa2307770
9. Burzotta F, Leone AM, Aurigemma C, et al. Fractional flow reserve or optical coherence tomography to guide management of angiographically intermediate coronary stenosis. *JACC: Cardiovasc Interv*. 2020;13(1):49-58. doi:10.1016/j.jcin.2019.09.034
10. Obermeyer Z, Emanuel EJ. Predicting the future - big data, machine learning, and clinical Medicine. *N Engl J Med*. 2016;375(13):1216-1219. doi:10.1056/NEJMp1606181
11. Chen JH, Asch SM. Machine learning and prediction in medicine - beyond the peak of inflated expectations. *N Engl J Med*. 2017;376(26):2507-2509. doi:10.1056/NEJMp1702071
12. Davenport T, Kalakota R. The potential for artificial intelligence in healthcare. *Future Hosp J*. 2019;6(2):94-98. doi:10.7861/futurehosp.6-2-94
13. Yu KH, Beam AL, Kohane IS. Artificial intelligence in healthcare. *Nat Biomed Eng*. 2018;2(10):719-731. doi:10.1038/s41551-018-0305-z
14. Lin A, Kolossv ary M, Motwani M, et al. Artificial intelligence in cardiovascular CT: current status and future implications.

- J Cardiovasc Comput Tomogr.* 2021;15(6):462-469. doi:10.1016/j.jcct.2021.03.006
15. Moons KGM, Altman DG, Reitsma JB, et al. Transparent reporting of a multivariable prediction model for individual prognosis or diagnosis (TRIPOD): explanation and elaboration. *Ann Intern Med.* 2015; 162(1):W1-W73. doi:10.7326/M14-0698
 16. Pawlowski T, Prati F, Kulawik T, Ficarra E, Bil J, Gil R. Optical coherence tomography criteria for defining functional severity of intermediate lesions: a comparative study with FFR. *Int J Cardiovasc Imaging.* 2013;29(8):1685-1691. doi:10.1007/s10554-013-0283-x
 17. Biały D, Wawrzyńska M, Arkowski J, et al. Multimodality imaging of intermediate lesions: data from FFR, OCT, NIRS-IVUS. *Cardiol J.* 2013;25(2):196-202. doi:10.5603/CJ.a2017.0082
 18. Burzotta F, Nerla R, Hill J, et al. Correlation between frequency-domain optical coherence tomography and fractional flow reserve in angiographically-intermediate coronary lesions. *Int J Cardiol.* 2018;253:55-60. doi:10.1016/j.ijcard.2017.10.011
 19. Wolfrum M, De Maria GL, Benenati S, et al. What are the causes of a suboptimal FFR after coronary stent deployment? insights from a consecutive series using OCT imaging. *EuroIntervention.* 2018; 14(12):e1324-e1331. doi:10.4244/EIJ-D-18-00071
 20. Paraggio L, Burzotta F, Aurigemma C, et al. Trends and outcomes of optical coherence tomography use: 877 patients single-center experience. *Cardiovasc Revasc Med.* 2019;20(4):303-310. doi:10.1016/j.carrev.2018.12.017
 21. D'Ascenzo F, Iannaccone M, De Filippo O, et al. Optical coherence tomography compared with fractional flow reserve guided approach in acute coronary syndromes: a propensity matched analysis. *Int J Cardiol.* 2017;244:54-58. doi:10.1016/j.ijcard.2017.05.108
 22. Usui E, Yonetsu T, Kanaji Y, et al. Optical coherence tomography-defined plaque vulnerability in relation to functional stenosis severity and microvascular dysfunction. *JACC: Cardiovasc Interv.* 2018;11(20):2058-2068. doi:10.1016/j.jcin.2018.07.012
 23. Belkacemi A, Stella PR, Ali DS, et al. Diagnostic accuracy of optical coherence tomography parameters in predicting in-stent hemodynamic severe coronary lesions: validation against fractional flow reserve. *Int J Cardiol.* 2013;168(4):4209-4213. doi:10.1016/j.ijcard.2013.07.178
 24. Leone AM, Porto I, De Caterina AR, et al. Maximal hyperemia in the assessment of fractional flow reserve. *JACC: Cardiovasc Interv.* 2012;5(4):402-408. doi:10.1016/j.jcin.2011.12.014
 25. Tearney GJ, Regar E, Akasaka T, et al. Consensus standards for acquisition, measurement, and reporting of intravascular optical coherence tomography studies. *J Am Coll Cardiol.* 2012;59(12): 1058-1072. doi:10.1016/j.jacc.2011.09.079
 26. Vergallo R, Lombardi M, Kakuta T, et al. Optical coherence tomography measures Predicting fractional flow reserve: the OMEF study. *J Soc Cardiovascular Angiogr Interven.* 2024;3:101288. doi:10.1016/j.jscv.2023.101288
 27. Pedersen A, Mikkelsen E, Cronin-Fenton D, et al. Missing data and multiple imputation in clinical epidemiological research. *Clin Epidemiol.* 2017;9:157-166. doi:10.2147/CLEP.S129785
 28. Graham JW. Missing data analysis: making it work in the real world. *Annu Rev Psychol.* 2009;60:549-576. doi:10.1146/annurev.psych.58.110405.085530
 29. Breiman L, Friedman JH, Olshen RA, Stone CJ. *Classification And Regression Trees.* Routledge; 2017. doi:10.1201/9781315139470
 30. Dudani SA. The Distance-Weighted k-Nearest-Neighbor rule. *IEEE Trans Syst Man Cybern.* 1976;SMC-6(4):325-327. doi:10.1109/TSMC.1976.5408784
 31. Hastie T, Buja A, Tibshirani R. Penalized discriminant analysis. *Ann Math Stat.* 1995;23(1):73-102. doi:10.1214/aos/1176324456
 32. Breiman L. Random forests. machine learning. *Mach Learn.* 2001;45(1):5-32. doi:10.1023/A:1010933404324
 33. Noble WS. What is a support vector machine? *Nat Biotechnol.* 2006;24(12):1565-1567. doi:10.1038/nbt1206-1565
 34. Friedman JH. Greedy function approximation: a gradient boosting machine. *Ann Stat.* 2001;29(5):1189-1232. doi:10.1214/aos/1013203451
 35. Chawla NV, Bowyer KW, Hall LO, Kegelmeyer WP. SMOTE: synthetic minority over-sampling technique. *J Artif Intell.* 2002;16: 321-357. doi:10.1613/jair.953
 36. Probst P, Wright MN, Boulesteix AL. Hyperparameters and tuning strategies for random forest. *Wires Data Min Knowl Discov.* 2019; 9(3):e1301. doi:10.1002/widm.1301
 37. Altmann A, Tološi L, Sander O, Lengauer T. Permutation importance: a corrected feature importance measure. *Bioinformatics.* 2010;26(10): 1340-1347. doi:10.1093/bioinformatics/btq134
 38. Neumann FJ, Sousa-Uva M, Ahlsson A, et al. 2018 ESC/EACTS guidelines on myocardial revascularization. *EuroIntervention.* 2019;14 (14):1435-1534. doi:10.4244/EIJY19M01_01
 39. Papafaklis MI, Muramatsu T, Ishibashi Y, et al. Fast virtual functional assessment of intermediate coronary lesions using routine angiographic data and blood flow simulation in humans: comparison with pressure wire—fractional flow reserve. *EuroIntervention.* 2014;10(5): 574-583. doi:10.4244/EIJY14M07_01
 40. Yu W, Huang J, Jia D, et al. Diagnostic accuracy of intracoronary optical coherence tomography-derived fractional flow reserve for assessment of coronary stenosis severity. *EuroIntervention.* 2019; 15(2):189-197. doi:10.4244/EIJ-D-19-00182
 41. Agarwal SK, Kasula S, Edupuganti MM, et al. Clinical Decision-Making for the hemodynamic “gray zone” (FFR 0.75-0.80) and long-Term outcomes. *J Invasive Cardiol.* 2017;29(11):371-376.
 42. Andreou C, Zimmermann FM, Tonino PAL, et al. Optimal treatment strategy for coronary artery stenoses with grey zone fractional flow reserve values. A systematic review and meta-analysis. *Cardiovasc Revasc Med.* 2020;21(3):392-397. doi:10.1016/j.carrev.2019.05.018
 43. Lee JG, Ko J, Hae H, et al. Intravascular ultrasound-based machine learning for predicting fractional flow reserve in intermediate coronary artery lesions. *Atherosclerosis.* 2020;292:171-177. doi:10.1016/j.atherosclerosis.2019.10.022
 44. De Bruyne B, Pijls NHJ, Kalesan B, et al. Fractional flow reserve-guided PCI versus medical therapy in stable coronary disease. *N Engl J Med.* 2012;367(11):991-1001. doi:10.1056/NEJMoa1205361
 45. Ying X. An overview of overfitting and its solutions. *J Phys: Conf Ser.* 2019;1168(2):022022. doi:10.1088/1742-6596/1168/2/022022
 46. Cawley GC, Talbot NLC. On over-fitting in model selection and subsequent selection bias in performance evaluation. *J Mach Learn Res.* 2010;11:2079-2107.
 47. Ha J, Kim JS, Lim J, et al. Assessing computational fractional flow reserve from optical coherence tomography in patients with intermediate coronary stenosis in the left anterior descending artery. *Circ Cardiovasc Interv.* 2016;9(8):e003613. doi:10.1161/CIRCINTERVENTIONS.116.003613
 48. Huang J, Emori H, Ding D, et al. Diagnostic performance of intracoronary optical coherence tomography-based versus angiography-based fractional flow reserve for the evaluation of coronary lesions. *EuroIntervention.* 2020;16(7):568-576. doi:10.4244/EIJ-D-19-01034
 49. Shew M, New J, Bur AM. Machine learning to predict delays in adjuvant radiation following surgery for head and neck cancer. *Otolaryngol Head Neck Surg.* 2019;160(6):1058-1064. doi:10.1177/0194599818823200
 50. Huynh-Thu VA, Saeys Y, Wehenkel L, Geurts P. Statistical interpretation of machine learning-based feature importance scores for biomarker discovery. *Bioinformatics.* 2012;28(13):1766-1774. doi:10.1093/bioinformatics/bts238

51. Mi X, Zou B, Zou F, Hu J. Permutation-based identification of important biomarkers for complex diseases via machine learning models. *Nat Commun.* 2021;12(1):3008. doi:10.1038/s41467-021-22756-2

SUPPORTING INFORMATION

Additional supporting information can be found online in the Supporting Information section at the end of this article.

How to cite this article: Lombardi M, Vergallo R, Costantino A, et al. Development of machine learning models for fractional flow reserve prediction in angiographically intermediate coronary lesions. *Catheter Cardiovasc Interv.* 2024;1-11. doi:10.1002/ccd.31167